

Research Article

Effect of Charging and Position of Metallic Particle Adhered to Spacer on PDIV and PRPD Characteristics in GIS

¹Y. Khan, ¹A.A. Khan, ¹F.N. Budiman, ^{1,2}A. Beroual, ¹N.H. Malik and ¹A.A. Al-Arainy

¹Saudi Aramco Chair in Electrical Power, Department of Electrical Engineering, College of Engineering, King Saud University, Riyadh, Saudi Arabia

²Ecole Centrale de Lyon, University of Lyon, AMPERE Lab CNRS UMR 5005, 30 Avenue Guy de Collongue, Ecully, France

Abstract: Gas Insulated Switchgears (GIS) are widely used due to their many benefits. The reliability of GIS is challenged due to the presence of spacer defects and/or metallic particles. Free metallic particles can tremendously reduce the insulation strength of GIS especially when they enter the triple junction region (consisting of the spacer, the electrode and the gaseous medium interface) around the spacer. Therefore, there is a need to investigate the effect of charged metallic particle on the field intensification produced along the spacer surface and its consequences on the Partial Discharge Inception Voltage (PDIV). In this study, simulation and experimental results are reported for metallic particles adhering to a cylindrical spacer. The effect of particle charging on the resulting field intensification, particle initiated partial discharge inception voltage as well as Phase Resolved Partial Discharge (PRPD) characteristics are presented in this study. The particle adversely affects the electric field uniformity in the area between the two electrodes. A particle in contact with the electrode causes the most severe intensification in the electric field, while the effect caused by the particle at the gap centre is the least severe.

Keywords: Charged particle, electric field, GIS, partial discharge, PDIV, PRPD, spacer

INTRODUCTION

Gas Insulated Switchgears (GIS) due to their many advantages are widely used in electrical power industry. In such equipments, spacers are used to support the High Voltage (HV) conductor and to maintain specified clearance between the HV conductor and the grounded enclosure. However, the spacers generally form the weakest link in GIS due to the field intensifications that occur at the triple junction. Similarly, field intensification also occurs on spacer surface due to spacer design, system configuration or spacer defects. SF₆ gas or its mixture with other gases used in GIS are highly sensitive to electric field intensification and the reliability of system (GIS) is challenged due to the presence of defects that cause microscopic regions at which the local electric field is enhanced resulting in partial discharge initiation, the intensification and development of which can lead to complete failure (CIGRE Working Group 01.03, 2004; Takuma *et al.*, 2000; Srivastava and Moncos, 2001; Braun *et al.*, 1993). Moreover the breakdown strength of GIS is strongly influenced by the roughness of the spacer surface and defects/protrusions produced from improper manufacturing (Srivastava and Moncos,

2001). GIS can be contaminated with non-conducting and conducting particles produced due to mechanical abrasion or arcing occurring during the operation of the isolating switches and circuit breakers. The effect of a particle depends on the type, size, shape, location as well as density of the particle. Studies conducted using scaled models and actual spacers with fixed particle on spacer surface verified that a drastic reduction occurs in the breakdown strength (Mazurek *et al.*, 1993; Hasegawa *et al.*, 2002). Therefore the knowledge of the electric field intensification around the conducting particles contributes towards a better understanding of the spacer surface flashover phenomenon.

When a metallic particle rests at the Grounded Electrode (GE), it has no surface charge density in the absence of electric field. However, in the presence of an electric field, free electrons inside the particle will move in such a way so as to oppose the external electric field. If there is no micro-discharge during the particle excursions, the net charge on the particle remains constant. However, a particle gets a new charge as soon as it touches an electrode.

The negative charge density induced on the particle surface is proportional to the applied electric field. When the applied field is increased, the negative charge

Corresponding Author: Y. Khan, Saudi Aramco Chair in Electrical Power, Department of Electrical Engineering, College of Engineering, King Saud University, Riyadh, Saudi Arabia

This work is licensed under a Creative Commons Attribution 4.0 International License (URL: <http://creativecommons.org/licenses/by/4.0/>).

density will also increase. Consequently, the electrostatic force (F_e) will increase and at the moment its value is higher than the gravitational force (F_g), the particle starts to lift-off the bottom surface and it moves in the direction of the electric field. Such a free charged particle can easily adhere to spacer due to mechanism explained next. When a charged particle is in contact with a spacer, an induced electrostatic force acts on it in a direction perpendicular to the spacer. In this case, if the frictional force between the particle and the spacer surface overcomes the gravitational force acting on the particle, the particle remains adhered to the spacer. Due to this reason, there is a definite possibility that a particle can adhere to the spacer surface.

In case of an AC electric field, the field direction changes every half cycle of power supply voltage. The particle moves between the electrodes. If the particle reaches and touches the opposite electrode, it will gain a new net charge which will make the force on particle to change its direction. Due to periodic polarity changing of the electric field, the particle motion in AC is more random. The new net charge after each consecutive impact of the particle to the GE will most likely be different. However the situation is different under DC electric field where once the particle lift-off, it will continuously move towards the opposite electrode.

Radwan *et al.* (2006a, b and 2007) and Khan *et al.* (2005, 2012) discussed the field distributions in cone shaped spacers and studied the effect of relative permittivity of spacer on the field distribution for cone and disc shaped spacers. However, spacer surface field distribution in the presence of charged or uncharged conducting particles needs further investigations. This study reports on the results of simulation and experimental studies when a conducting metallic particles adheres to a disc shaped spacer. The effects of field intensifications on Partial Discharge Inception Voltage (PDIV) and Phase Resolved Partial Discharge (PRPD) characteristics are presented in this study.

The mobility of a particle is also influenced by its shape. An elongated particle is more mobile than a spherical particle (CIGRE Working Group D1.33, 2008). This is due to the charge-to-mass ratio, which for an elongated particle is greater than for a spherical particle. To estimate the particle's net charge in a GIS, the formulation proposed in Malik and Qureshi (1979) is widely used. In these equations, it is assumed that the time needed to rearrange the charges on the particle surface is negligible. The formulae are valid as long the particle is metallic and in good contact with the electrode. For a wire shaped particle the formulas for charge calculation in horizontal and vertical positions are given as (Malik and Qureshi, 1979):

$$Q_h = 2\pi\epsilon_0 r l E \quad (1)$$

$$Q_v = \frac{\pi\epsilon_0 l^2 E}{\ln\left(\frac{2l}{r}\right) - 1} \quad (2)$$

where, Q_h is charge of particle in horizontal position, Q_v is the charge of particle in vertical position, r and l are the radius and the length of the cylindrical shaped wire particle, ϵ_0 is the absolute dielectric permittivity and E is the applied electric field. It should be noted that in the vertical formulation, the particle is assumed to have a semi-ellipsoid shape.

METHODOLOGY

GIS system model: The investigated model shown in Fig. 1 consists of two parallel-plane stainless-steel electrodes separated by a Plexiglas cylindrical shaped spacer of 15 mm diameter and 15 mm length. A defect was created by gluing a cylindrical stainless-steel particle of $\phi = 0.5$ mm diameter and $L = 2$ mm length on the spacer surface. The parameter H defines the distance between the bottom tip of particle and the surface of grounded electrode and its values were chosen to result in particle at the gap center, touching either of the electrodes and between the gap center and the electrode surface. Thus for $L = 2$ mm long particle H had values of 0, 3.25, 6.5, 9.75 and 13 mm, respectively. For the experimental measurements, SF₆ gas was maintained at a pressure of 1 bar.

Ansoft's Maxwell v14 software was used to perform the numerical analysis of the electrostatic field distribution with/without particle. Subsequently, the computed electric field values were used to estimate the PDIV in the presence of particle on the spacer surface. The estimated PDIV values were confirmed by experimental measurements performed using IEC 60270 method (Magnus, 1997). In the experimental measurements of PDs, Hipotronics DDX-7000 Digital PD detector was used.

Electrostatic simulation: Electrostatic simulations were performed to study the field intensification produced by the presence of uncharged and charged metallic particles adhering to the spacer surface. For these simulations, the HV electrode was assumed at +30kV. In order to study the effect of charged particle on electric field intensification, a charge of ± 9 nC was selected.

In the absence of such a particle, the electric field along the spacer surface will be roughly uniform within the electrodes gap. The electric field E without particle was 2.0×10^6 V/m. In this case, the PDIV value will correspond to the spacer flashover voltage since discharge inception will lead to complete flashover of the spacer. However, when the uncharged particle is present, the electric field will be distorted resulting in a region of field intensification. However, as expected the extent of field intensification depends on particle dimensions, position on the spacer, value of the applied voltage, the polarity and magnitude of the

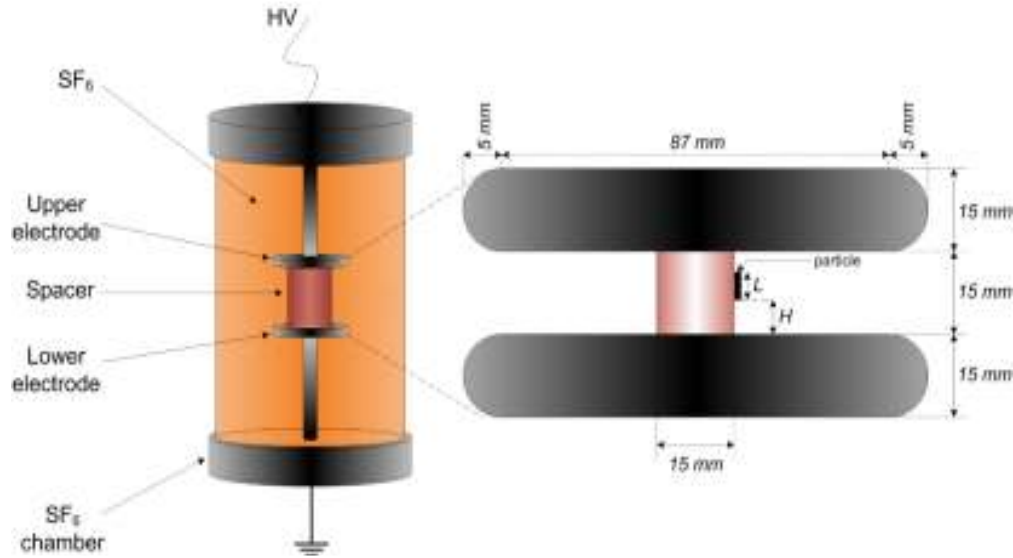


Fig. 1: The test system

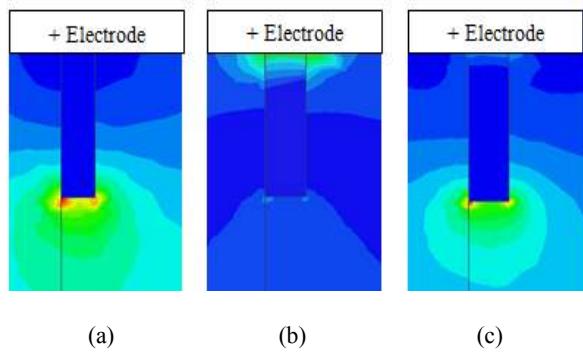


Fig. 2: Field intensification pattern in case of, (a) positive charged particle, (b) negative charged particle, (c) uncharged particle

electrical charge on particle, etc. Figure 2 shows the field intensification patterns when charged or uncharged particle is present at the HV electrode.

Table 1 and 2 shows the maximum and average electric field values along the spacer surface. Table 3 shows the maximum electric field values for the two cases to show the field intensification in the presence of a micro gap between the charged/uncharged particle and the electrode. The micro-gap in this case is assumed as 0.05 mm to either the HV electrode or the grounded electrode. Due to extremely high electric field in the presence of micro-gap, breakdown occurs when a particle is approaching the opposite electrode that initially leads to a micro-discharge which eventually transforms into a complete breakdown.

The electric field calculation: The purpose of this calculation was to map the electric field distribution over the entire region between the two electrodes, since

Table 1: Maximum electric field E (V/m) values for different particle positions when $L = 2 \text{ mm}$, $\phi = 0.5 \text{ mm}$ and $V = 30 \text{ kV}$

Particle position	Uncharged	Positive charged	Negative charged
H (mm)			
1	7.800×10^6	-	-
2	7.785×10^6	1.483×10^7	8.579×10^6
3	6.266×10^6	1.100×10^7	1.095×10^7
4	7.178×10^6	1.534×10^7	1.987×10^7
5	7.800×10^6	-	-

Table 2: Average electric field E (V/m) values for different particle positions

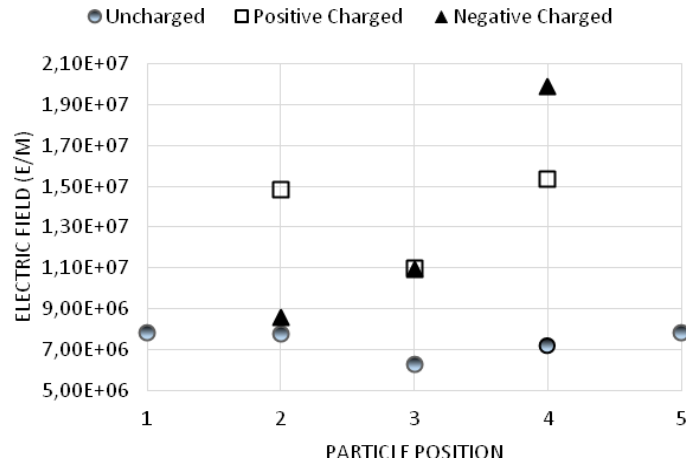
Particle position	Uncharged	Positive charged	Negative charged
H (mm)			
2	2.193×10^6	2.291×10^6	2.239×10^6
3	2.194×10^6	2.272×10^6	2.257×10^6
4	2.203×10^6	2.259×10^6	2.298×10^6

Table 3: Maximum electric field E (V/m) in the presence of micro-gap (0.05 mm) between the particle and the electrode

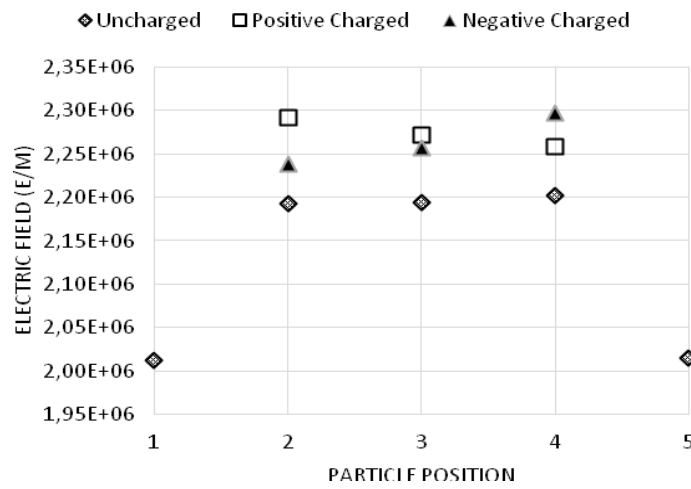
Particle position	Uncharged	Positive charged	Negative charged
H (mm)			
0.05	7.800×10^6	4.162×10^7	1.067×10^7
14.95	1.724×10^7	1.084×10^7	4.163×10^7

it helps in determining the area within the region with the highest likelihood of PD occurrence.

In the absence of any particle, the electric field across the spacer surface is uniform at $2 \times 10^6 \text{ V/m}$. However, introduction of particle distorts the field. In case of uncharged particle, the highest field intensity considering all the particle positions was $\sim 7 \times 10^6 \text{ V/m}$ while the average electric field was $\sim (2 \text{ to } 2.2) \times 10^6 \text{ V/m}$. In case of positive charged particle, the average electric field dropped from $2.3 \times 10^6 \text{ V/m}$ at position 2, to $2.26 \times 10^6 \text{ V/m}$ at position 4. However, in case of negative charged particle, the electric field increased from $2.24 \times 10^6 \text{ V/m}$ at position 2, to $2.4 \times 10^6 \text{ V/m}$ at position 4. Among all the cases investigated, the highest electric field was noted due to negative charged particle



(a) Maximum electric field for different locations



(b) Average electric field

Fig. 3: Electric field values of different locations of charged and uncharged particle

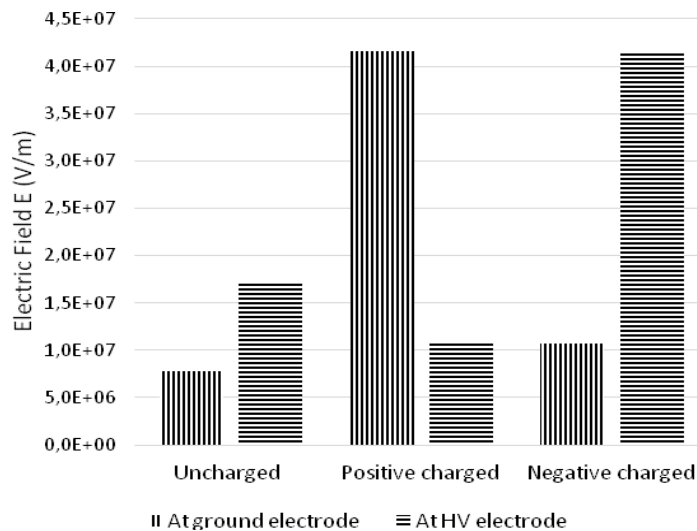


Fig. 4: Maximum field intensity when particle is 0.05 mm away from electrodes

Table 4: Field utilization factor (u) values for different positions, particle charge: $\pm 9\text{nC}$

Position H (mm)	Uncharged	Positively charged	Negatively charged
1	0.258	-	-
2	0.282	0.154	0.261
3	0.350	0.206	0.206
4	0.307	0.147	0.116
5	0.258	-	-

Table 5: Field utilization factor (u) values when particle is 0.05 mm away from either electrode: (particle charge: $\pm 9\text{nC}$)

Position H (mm)	Uncharged	Positively charged	Negatively charged
0.05	0.258	0.049	0.211
12.95	0.117	0.189	0.049

at position 4 where the electric field was around 1.99×10^7 V/m. The maximum electric field in case of negative charged particle is 2.55 times while that for positive charged particle is 1.96 times the maximum electric field in case of uncharged particle as clear from Fig. 3 and 4. Therefore, the PDIV values in case of charged particle are expected to be lower than those for uncharged particle.

When particle is present 0.05 mm away from the electrode, significant field intensification is observed. For uncharged particle, field intensity is greater at HV electrode as compared to that at Grounded Electrode (GE). However, as expected, for positive charged particle, the maximum field is observed at GE while in case of negative charged particle, the electric field is highest at the HV electrode as shown in Fig. 4.

The electric field utilization factor (u): The electric field utilization factor (u) is defined as the ratio between the average electric field and the maximum electric field in the gap. Thus, the value of u is always ≤ 1 . This factor is used to express the degree of field non-uniformity caused by a conducting particle in the studied system. The lower the value of u , the higher will be the degree of field non-uniformity. Field intensification f is related to the utilization factor as $f = 1/u$.

The procedure used for calculating the field utilization is summarized here. The area where electric field was evaluated was area between the electrodes and had the size of $87 \times 15 \text{ mm}^2$. It was divided into many sub-areas (rectangles) of dy -length and dx -width. In order to achieve high accuracy, dx and dy were made very small such that, $dx = dy = 0.1 \text{ mm}$. The electric fields on all corner points of each sub-area were evaluated and tabulated. In this way, the number of evaluated points for each simulation became 131521. The field utilization factor was then simply calculated as the ratio between the average field value and the maximum field value.

Table 4 and 5 report the values of the u for different cases. It can be noticed that utilization factor is lower in case of charged particle as compared to it values in case



Fig. 5: Experimental setup established in the laboratory



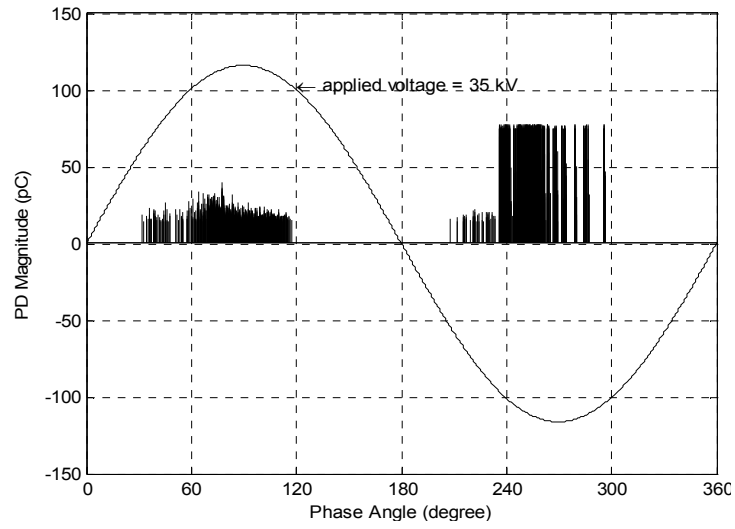
Fig. 6: Spacers with attached particles

of uncharged particle. However, the utilization factor values are even lower when a micro-gap is present between the particle and the electrode thus increasing the chance of PD occurrence at lower PDIV values compared to the other cases. It should be noted that it has been observed experimentally, that the particle initiated breakdown in SF_6 triggers when a particle approaches, but is not in contact with the opposite electrode. It is believed that spacer present a similar behavior will be observed.

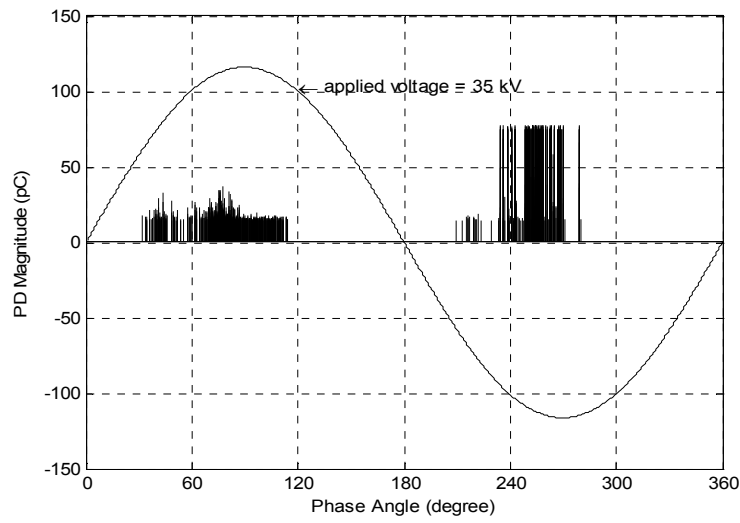
EXPERIMENTAL RESULTS

Experiments were also performed using the same setup as described in Fig. 1. For each particle position on the spacer, the experiments were repeated several times. Figure 5 shows the actual experimental setup established in laboratory while Fig. 6 shows the photographs of spacers with particles adhered on surface at different positions. IEC PD measuring system was connected to acquire the discharge patterns and to measure partial discharge inception voltages for each case. SF_6 was maintained at 1 bar pressure for all the experiments when recording the PD pattern and PDIV values.

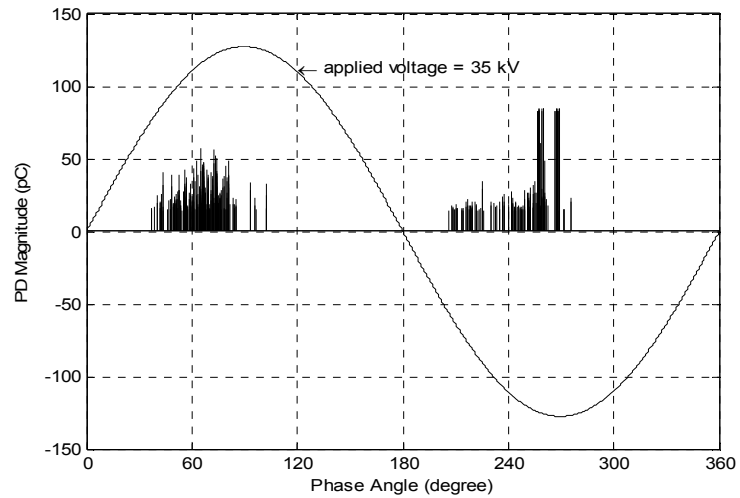
In order to investigate the dependence of PD magnitude and pattern on the particle position on the spacer surface, PRPD (ϕ - q characteristic) patterns for



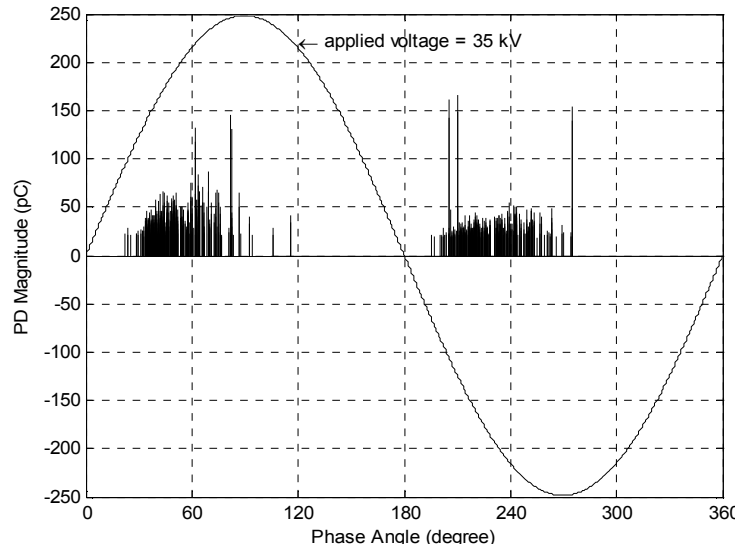
(a) H = 0 mm



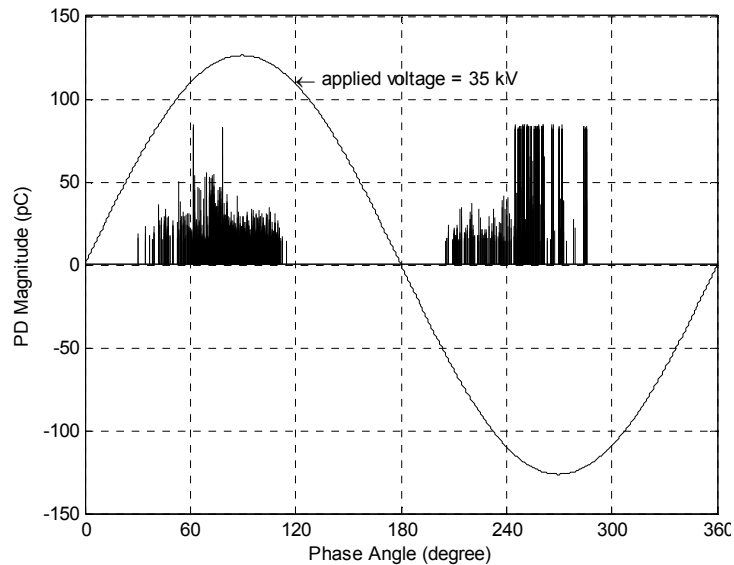
(b) H = 3.25 mm



(c) H = 6.5 mm



(d) H = 9.75 mm



(e) H = 13 mm

Fig. 7: PRPD patterns for all particle positions on the spacer surface (sampling time: 20 sec)

each particle position were established and the results are shown in Fig. 7.

DISCUSSION

This section briefly discusses the results obtained from the simulations and experiments. The discussion also includes the utilization of estimated electric field to estimate PDIV values in the modelled system.

The estimation of PDIV values: In SF₆ gas both the ionization co-efficient α and attachment co-efficient η depend upon the values of (E/p) , where E is electric

field and p is gas pressure (in bar). The PDIV values can be estimated using the following formula (Malik and Qureshi, 1979; Hayakawa *et al.*, 2008):

$$V_{Pd} = (E/p)_{lim} \cdot u \cdot p \cdot (d - L) \quad (3)$$

where, V_{Pd} is the estimated PDIV value (in kV_{peak}), $(E/p)_{lim}$ is the critical value of the pressure-reduced electric field (in kV/cm) in SF₆, at which $\alpha = \eta$. $(E/p)_{lim}$ is equal to 87.75 kV/(cm-bar), u is the field utilization factor of the system, d (in cm) is the total gap length and L (in cm) is the particle length. For $(E/p) < (E/p)_{lim}$, since $\alpha < \eta$ and thus there is no chance of any breakdown. Thus the

lowest value of voltage at which discharge can initialize will be the PDIV.

Using Eq. (4), it is found that the estimated PDIV values when particle is in contact with the electrode is ~29.4 kV while the experimental values for PDIV was ~30 kV when the particle is either in contact with HV electrode or the grounded electrode. Thus, the calculated values are very close to experimental results for PDIV values with an error of ~2%. Therefore, for the cases where the field utilization factor value is lower than 0.258 (for uncharged particle at $H = 0$ mm or $H = 13$ mm), lower PDIV values are expected theoretically. There were some cases in which the PDIV values were lower than 30 kV. One of the reason that can be predicted from the simulation results and discussions, can be due to charging phenomenon of particle that rises the electric field reducing the PDIV values.

When particle is charged, u will depend on the value and polarity of charge also. Therefore, in such a case, PDIV values are expected to change with the value and polarity of charge. Such a behavior has been experimentally studies and reported in Hayakawa *et al.* (2008) and Mansour *et al.* (2010). A further observation is that if a charged particle approaches the opposite polarity electrode, the value of u becomes very small as shown in Table 6, thus the PDIV values will significantly decrease. Hence a micro discharge is expected to initiate at lower voltage in such cases. In studies with free conducting particles, such behavior has been reported in the literature.

Table 6: Experimental values of PDIV for different particle position ($L = 2$ mm, $\phi = 0.5$ mm) at $P = 1$ bar

H (mm)	PDIV (kVrms)		
	Min.	Max.	Avg.
0	29.06	30.51	29.85
3.25	32.30	32.60	32.50
6.50	31.51	32.30	31.77
9.75	32.01	33.10	32.50
13	29.82	30.50	30.36

Min.: Minimum; Max.: Maximum; Avg. Average

Effect of particle position on the PD pattern: The relationship between particle position and PD pattern shown in Fig. 7 can be characterized by comparing the total PD charge magnitude occurring in the positive half-cycle with that occurring in the negative half-cycle. When the particle is in contact with the GE (i.e., $H = 0$ mm), PD occurrence in the negative half-cycle has a higher total charge magnitude. Meanwhile, the ratio between the total PD charge magnitude in the negative half-cycle and the total PD charge magnitude in the positive half-cycle becomes lower when the particle is located between the lower electrode and the gap center (i.e., $H = 3.25$ mm). As the particle location is shifted towards the HV electrode, the total PD charge magnitude in the positive half-cycle becomes higher as compared to the one in the negative half-cycle.

The relationship described above is further depicted by Fig. 8. This figure clearly shows the effect of particle position on the percentage of the total PD charge magnitude in each half-cycle of the applied voltage. When the particle is below the gap center, a higher PD magnitude occurs in the negative half-cycle. The highest percentage, which is 65.54%, is achieved when the

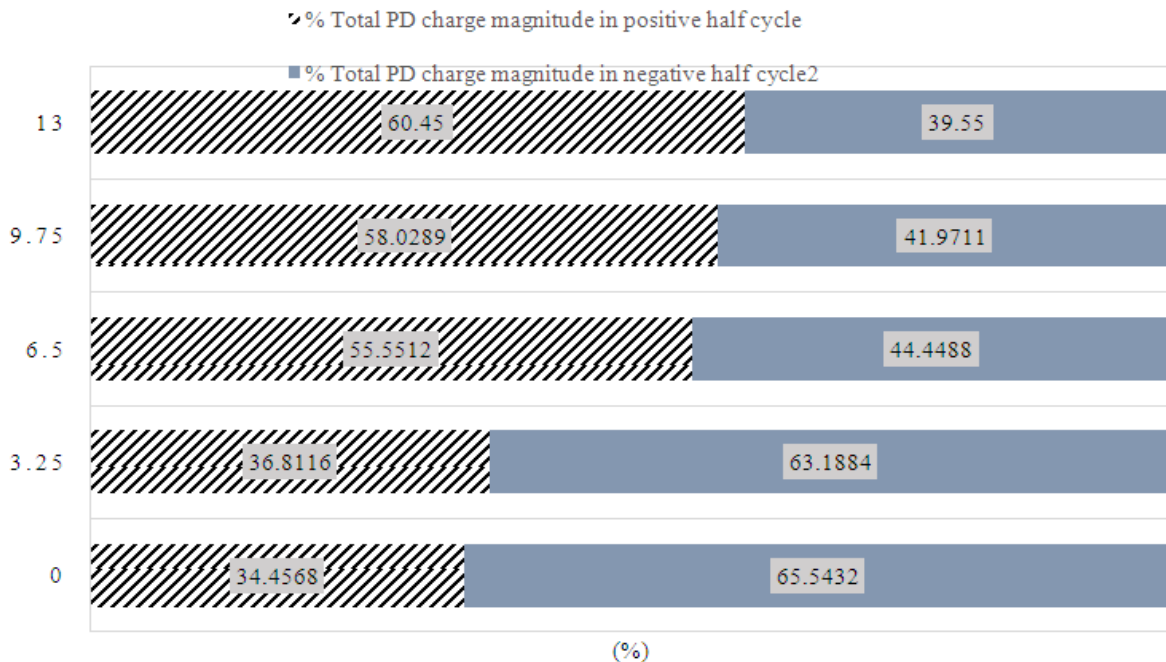


Fig. 8: Distribution of PD charge magnitude in each half-cycle of the applied voltage expressed as percentages of the total PD charge magnitude

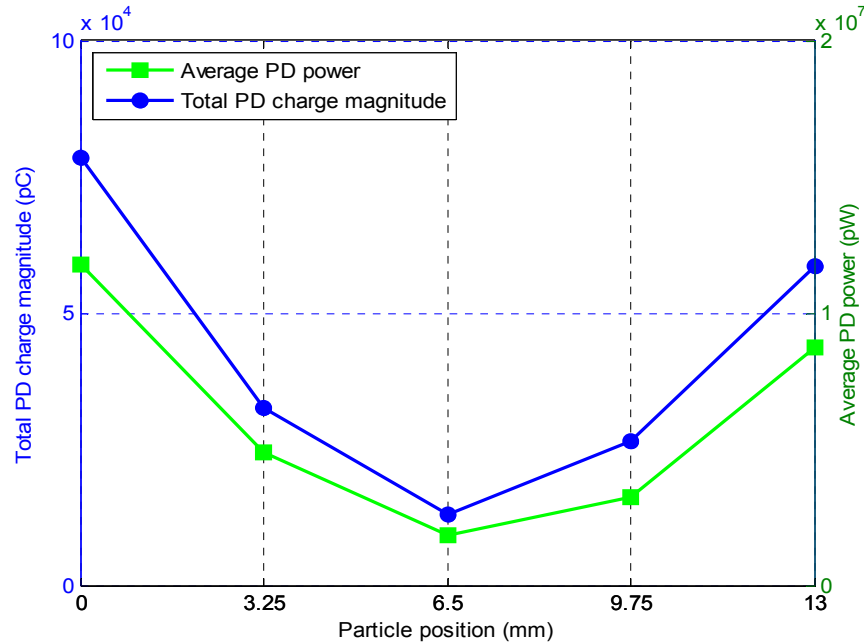


Fig. 9: The relationship between two PD quantities (total PD charge magnitude and average PD power) and particle position

particle touches the lower electrode. Conversely, PD with a higher magnitude in the positive half-cycle is obtained when the particle adheres to the spacer above the gap center. In case of the contact between particle and the high voltage electrode, the highest percentage 60.45% is achieved. When the particle is placed on the gap center, the total PD charge magnitude in the positive half-cycle is slightly higher than that in the negative half-cycle. However, the ratio is lower when compared to the other cases, in which the particle is at a location other than the gap center.

Figure 9 presents the total PD charge magnitude and the average PD power as function of particle positions. As can be observed, both quantities have the same patterns. The lowest value is obtained when the particle is at the gap center, while the highest value is achieved when the particle is in contact with one of the electrodes. In this case, the contact between the particle and the ground electrode gives the highest value.

CONCLUSION

The effect of metallic particle adhering to the spacer surface in GIS on the electric field distribution as well as PDIV around the spacer was simulated and measured. The following conclusions can be drawn:

- The particle adversely affects the electric field uniformity in the area between the two electrodes. A particle in contact with the electrode causes the most severe intensification in the electric field, while the effect caused by the particle at the gap centre is the least severe.

- The electric field values were higher for charged particles as compared to the uncharged particles. Hence charging of particle will lead to changes in PDIV values than expected for uncharged particle cases.
- A good agreement is found between the estimated and the measured values of PDIV when the uncharged particle is in contact with either the HV or the ground electrode.

ACKNOWLEDGMENT

The authors are grateful to National Plan for Science and Technology (NPST), King Saud University Riyadh, Saudi Arabia for their technical and financial support provided through their research project # 08-ENE216-02.

REFERENCES

- Braun, J.M., G.L. Ford, N. Fujimoto, S. Riuetto and O.C. Stonet, 1993. Reliability of GIS EHV epoxy insulators: The need and prospects for more stringent acceptance criteria. IEEE T. Power Deliver., 8(1): 121-131.
- CIGRE Working Group 01.03, 2004. N₂/SF₆: Mixture for gas insulated systems. CIGRE-Report DI-201, Paris.
- CIGRE Working Group D1.33, 2008. Guide for electrical partial discharge measurements in compliance to IEC 60270. Technical Brochure, Electra, pp: 61-67.

- Hasegawa, T., K. Yamaji, M. Hatano, F. Endo, T. Rokunohe and T. Yamagiwa, 2002. Development of insulation structure and enhancement of insulation reliability of 500kV DC GIS. *IEEE T. Power Deliver.*, 12(1): 194-202.
- Hayakawa, N., T. Okusu, N. Kanako, H. Kojima, F. Endo, M. Yoshida, U. Katsumi and H. Okubo, 2008. Dependence of partial discharge characteristics at spacer surface on particle size in SF₆ gas insulated system. *Proceeding of the International Conference on Condition Monitoring and Diagnosis*. Beijing, China, pp: 46-50.
- Khan, Y., S. Okabe, J. Suehiro and M. Hara, 2005. Proposal for new particle deactivation methods in GIS. *IEEE T. Dielect. El. In.*, 12(1): 147-157.
- Khan, A.A., Y. Khan, N.H. Malik and A.A. Al-Arainy, 2012. Influence of spacer defects and adhered metal particles on electric field intensifications in GIS. *J. Basic. Appl. Sci. Res.*, 2(8): 7866-7875.
- Magnus, H., 1997. Motion of metallic particles in gas insulated systems. Ph.D. Thesis, Department of Electric Power Engineering, Chalmers University, Sweden.
- Malik, N.H. and A.H. Qureshi, 1979. Calculation of discharge inception voltages in SF₆-N₂ mixtures. *IEEE T. Electr. Insul.*, El-14(2): 70-76.
- Mansour, D.E.A., K. Nishizawa, H. Kojima, N. Hayakawa, F. Endo and H. Okubo, 2010. Charge accumulation effects on time transition of partial discharge activity at GIS spacer defects. *IEEE T. Dielect. El. In.*, 17(1): 247-255.
- Mazurek, B., J.D. Cross and R.G. Van Heeswijk, 1993. The effect of a metallic particle near a spacer on flashover phenomena in SF₆. *IEEE T. Dielect. El. In.*, 28(2): 219-229.
- Radwan, R.M. and A.M. Abou-Elyazied, 2006a. Electric Field Distribution on Insulating Spacers in GIS Using the Finite Element Technique. *CIGRE Paper A3-104*.
- Radwan, R.M. and A.M. Abou-Elyazied, 2006b. Effect of solid spacers' dimensions and permittivity on the electric field distribution in gas insulated systems. *Proceeding of the 11th International Middle East Power Systems Conference (MEPCON, 2006)*. El-Minia, pp: 234-239.
- Radwan, R.M. and A.M. Abou-Elyazied, 2007. Effect of spacer's defects and conducting particles on the electric field distribution along their surfaces in GIS. *IEEE T. Dielect. El. In.*, 14(6): 1484-1491.
- Srivastava, K.D. and M.M. Moncos, 2001. A review of some critical aspects or insulation design of GIS/GIL systems. *Proceeding of the IEEE Transmission and Distribution Conference*. Atlanta, USA, 2: 787-792.
- Takuma, T., F. Endo, H. Hama, S. Matsumoto and M. Yuhima, 2000. Interfacial insulation characteristics in gas mixtures as alternative to SF₆ and application to power equipment. *CIGRE Paper No. I5-207*.